

Terahertz Emission From Magneto-plasma Oscillations in Semiconductors

J. N. Heyman^{*a}, H. Wrage^a, C. Lind^a, D. Hebert^a, P. Neocleous^a,
P.A. Crowell^b, T. Müller^c, K. Unterrainer^c.

^aDept. of Physics and Astronomy, Macalester College; ^bDept. of Physics, University of Minnesota;

^cInstitute for Solid State Electronics, Technical University of Vienna.

ABSTRACT

Ultrafast terahertz spectroscopy can be used to probe charge and spin dynamics in semiconductors. We have studied THz emission from bulk InAs and GaAs and from GaAs/AlGaAs quantum wells as a function of magnetic field. Ultrashort pulses of THz radiation were produced at semiconductor surfaces by photoexcitation with a femtosecond Ti-Sapphire laser, and we recorded the THz emission spectrum and the integrated THz power as a function of magnetic field and temperature. In bulk samples the emitted radiation is produced by coupled cyclotron-plasma oscillations: we model THz emission from n-GaAs as magneto-plasma oscillations in a 3-D electron gas. THz emission from a modulation-doped parabolic quantum well is described in terms of coupled intersubband-cyclotron motion. A model including both 3-D plasma oscillations and a 2-D electron gas in a surface accumulation layer is required to describe THz emission from InAs in a magnetic field.

keywords: terahertz, ultrafast, InAs, GaAs, plasmon, magnetic, parabolic quantum well

I. INTRODUCTION

Ultrafast photoexcitation of semiconductor surfaces is a convenient, widely used technique for generating THz pulses.[1] The efficiency of this process can be increased by using a magnetic field to increase the component of the oscillating electric dipole perpendicular to the THz beam.[2] Sarakura et. al. [3] reported a substantial enhancement of the efficiency of THz generation at InAs surfaces by a moderate magnetic field, and average emitted THz powers of ~ 0.7 mW using a 1 W average power Ti-Sapphire pump laser. However, recent studies by McLaughlin, et. al.[4] and by ourselves [5] yield much lower, although still substantial THz powers of order ~ 10 μ W under similar experimental conditions. Ohatake et. al. has investigated the THz emission from InAs for a wide variety of magnetic field geometries.[6] Weiss, et. al. have investigated THz generation from InAs and a number of other semiconductors.[7] They show that the component of the power due to magnetic field varies as the square of the field for fields $B < 1$ T. A recent study by Corchia, et. al. [8] examines THz generation in GaAs in a magnetic field. They are able to successfully describe the dependence of the emitted THz power on magnetic field, and also the dependence of the THz emission on pump intensity. Recently, we have investigated THz emission from bulk InAs and GaAs as a function of magnetic field [5]. In this paper we summarize that work, and in addition report the magnetic field dependence of THz emission from a modulation-doped GaAs/AlGaAs parabolic quantum well. THz emission from n-GaAs in a magnetic field can be described as coupled plasma-cyclotron oscillations, and we model THz emission from the quantum well as coupled cyclotron-intersubband plasma oscillations of a 2D-electron gas. N-type InAs is a complicated system, containing both extrinsic electrons and a natural surface electron accumulation layer. We show that THz emission in n-InAs can be modeled as the sum of two components: coupled plasma-cyclotron oscillations from extrinsic carriers and cyclotron-intersubband oscillations from carriers in a 2D layer. Finally, we show that THz charge oscillations in InAs are excited by diffusion of photoexcited hot carriers rather than drift in the surface electric field.

*heyman@macalester.edu; phone 1 651 696-6369; fax 1 651 696 6122, Macalester College 1600 Grand Ave., St. Paul MN USA 55105.

2. MODEL

THz charge oscillations at semiconductor surfaces are initiated by ultrafast photoexcitation. In many III-V semiconductors the excitation mechanism is ultrafast screening of the surface electric field. More generally, photoexcitation produces a non-equilibrium concentration of hot carriers in the near surface region which drives diffusion. For electrons the electromotive force is

$$\varepsilon = E + Q\nabla T + \frac{eD_n}{\sigma} \nabla n \quad (1)$$

where σ is the conductivity, Q is the thermopower coefficient, and D_n is the electron diffusion coefficient. Although the second and third terms lead to a bipolar current, they do create a net electric field (a Dember field) because the diffusion coefficients of electrons and holes are not equal. It has been shown[9] that diffusion of hot carriers drives THz emission in the narrow-gap semiconductor Te, and we show below that this mechanism also drives THz emission in InAs.

Following initial excitation, it is found that n-type GaAs and InAs samples in zero magnetic field emit THz radiation at the plasma-frequency of the extrinsic electrons [10] [11]. Recently, we have used a semi-classical model of plasma-oscillations of electrons in a magnetic field to describe THz emission from GaAs and InAs.[5] We numerically solve the equations of motion, assume an impulsive excitation and calculate the response of the system in the long-wavelength limit ($q = 0$). THz emission from the oscillating plasma is calculated in the electric dipole approximation.

For bulk samples, the model predicts that electrons moving parallel to \mathbf{B} oscillate at the classical plasma frequency, while carrier motion perpendicular to \mathbf{B} couples into the high frequency and low frequency magnetoplasma modes. The origin of these modes can be easily understood: For $B = 0$, displacement of charge produces a linear restoring force through the space charge field. The in-plane equations of motion are identical to those of a 2-D harmonic oscillator, and two degenerate, independent solutions describe clockwise and counter-clockwise circular motion. A magnetic field perpendicular to the plane lifts the degeneracy. For a homogeneous 3-D electron plasma, the eigenvalues are

$$\begin{aligned} \omega_{\pm} &= \frac{1}{2} \left[(\omega_c + i\gamma) \pm \sqrt{(\omega_c + i\gamma)^2 + 4\omega_p^2} \right] & \mathbf{v} \perp \mathbf{B} \\ \omega_{\parallel} &= \omega_p, & \mathbf{v} \parallel \mathbf{B} \end{aligned} \quad (2)$$

where ω_c is the cyclotron frequency and ω_p is the plasma frequency.

We treat THz emission from a parabolically confined 2-D plasma by introducing a harmonic potential perpendicular to the surface. In addition, we assume that no space-charge field is created by motion of the 2-D electrons parallel to the surface in the long-wavelength limit. The eigenmodes are characteristic of coupled harmonic oscillators at $\omega_c \cos\theta$ and ω_s , where ω_s is the frequency for oscillations perpendicular to the surface and θ is the angle which \mathbf{B} makes with the surface normal. For a magnetic field *parallel* to the surface ($\theta = 0$), the response consists of a high-frequency mode at $\omega_+ = \sqrt{\omega_s^2 + \omega_c^2}$ and a low frequency mode at $\omega_- = 0$. Charge in the ω_- mode does not oscillate, but does emit low-frequency radiation as it decelerates due to damping.

3. EXPERIMENT

Optically pumped THz emission was measured in the reflection geometry. Pump radiation was incident at 45 degrees to the sample surface, and THz radiation was collected along the direction of the reflected pump pulse. Measurements were performed with the sample surface parallel to and at 45° to the magnetic field. For most measurements the samples were mounted in a horizontal split-coil superconducting magnet with a variable temperature insert (4-300K), and the pump was a 140fs mode-locked Ti:Sapphire laser oscillator. Since the excitation pulse-width sets an upper limit to the

emission frequencies observed in these experiments, we performed additional measurements using a 12fs Ti-Sapphire laser. For these measurements, samples were held at room temperature in air, and a permanent magnet was used to obtain magnetic fields of $\pm 0.5\text{T}$.

The samples investigated included bulk n-GaAs, bulk InAs (n-type and p-type), and a modulation-doped AlGaAs/GaAs parabolic quantum well ($n = 5 \cdot 10^{11} \text{cm}^{-2}$). The emission was recorded as a function of temperature between 280K and 10K. In bulk samples we observed a moderate temperature dependence to the emission. The quantum well sample was studied at $T = 10\text{K}$.

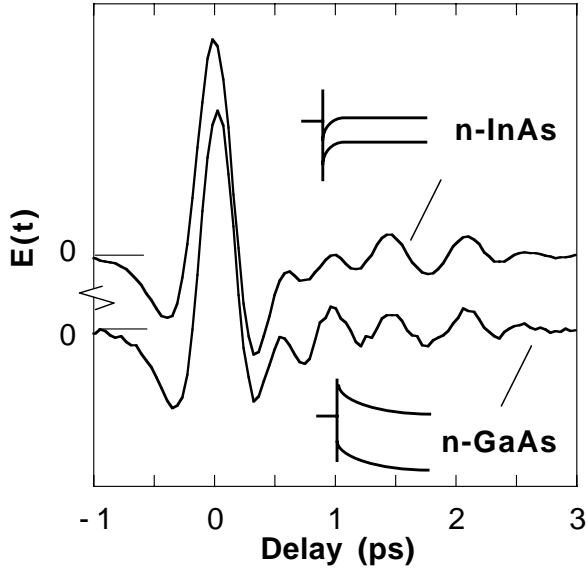


Fig. 1. THz emission from n-InAs ($n = 1.8 \times 10^{16} \text{cm}^{-3}$) and n-GaAs ($n = 1 \times 10^{17} \text{cm}^{-3}$) measured by electro-optic sampling. Although the surface electric field in the samples are in opposite directions, the initial sign of the THz electric field is the same. The waveforms have been normalized.

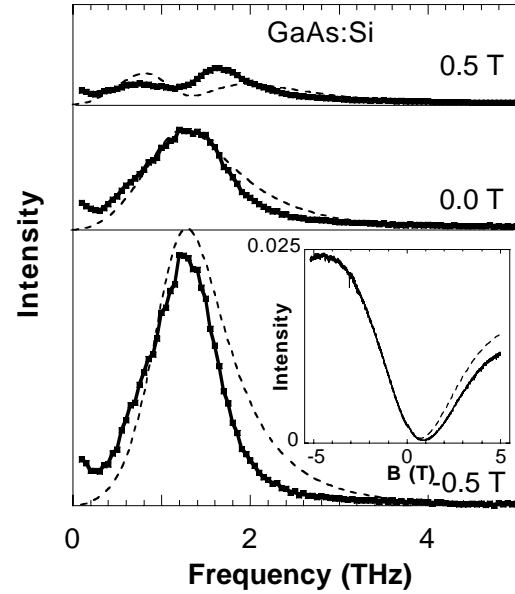


Fig. 2. THz emission spectrum of n-GaAs ($n = 2.4 \times 10^{16} \text{cm}^{-3}$) optically excited with a 12fs Ti:S laser. Solid lines are experimental data, dashed lines are fits to our model. Inset: integrated power versus magnetic field measured with a 140fs Ti:S laser.

3.1 n-GaAs

The zero-field THz emission spectrum of n-GaAs measured with the 12fs pump laser consists of a single broad peak centered at the plasma frequency. A sharp feature near the GaAs LO-phonon frequency is also observed. At positive magnetic fields parallel to the surface the plasma peak splits into two broad features which are distinct up to $B = 1.5\text{T}$. For negative fields in this same range, the two features are not distinct. Overall, the center frequency of the response shifts to lower frequencies at high fields. The THz power versus field is plotted in the inset to Figure 1. Interestingly, the minimum response is at $B = 0.9\text{T}$ rather than at $B = 0$. Our phase-sensitive detection technique shows that the electric field component at the zero-field plasma frequency changes sign at this minimum point.

In GaAs, we obtain good quantitative agreement between the model and experiment. Qualitatively, the field-dependence of the power arises from a geometrical effect: the curvature of the electron trajectories changes the component of the dipole moment perpendicular to outgoing THz beam. Since the sign of the change depends on the field direction, and because the dipole has a perpendicular component even at $B = 0$ in our geometry, the minimum intensity does not occur at zero-field. At high fields ($\omega_c \gg \gamma$), the electron trajectories are more nearly circular, so that geometrical effects become less important. In this regime, changes in the power reflect the field-dependence of the emission spectrum.

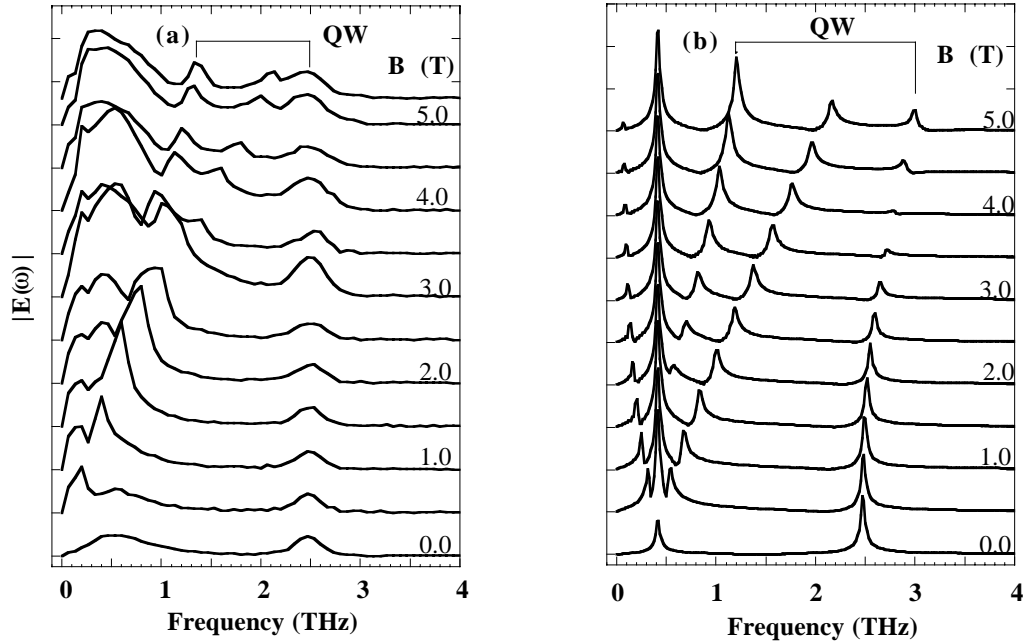


Fig. 3. (a) AlGaAs/GaAs parabolic quantum well: THz electric field amplitude versus frequency as a function of magnetic field from $B = 0$ to 5 T at 0.5T intervals, and 5.3T. (B at 45° to surface, $T = 10\text{K}$). Curves offset for clarity. (b) Simulated emission spectra. Model includes quantum well electrons in a parabolic potential, plus emission from photogenerated plasma ($n = 2 \cdot 10^{15} \text{cm}^{-3}$).

We can also give a physical basis for the magnetic field dependence of the emission spectrum. Under certain conditions, we can expect to resolve the upper and lower magneto-plasma modes in our measurements. While the dipole moment associated with the upper and lower modes oscillate in phase for very small fields, the contribution from one will change sign as the field is increased, with the lower (upper) mode changing sign at greater positive (negative) fields. This sign change is observed experimentally. When the dominant low frequency mode is suppressed near this sign change, the experimental data clearly show both modes. We conclude that THz emission from n-GaAs in a magnetic field is dominated by bulk magneto-plasma oscillations of the extrinsic carriers.

3.2 AlGaAs/GaAs Parabolic QW

THz emission from parabolic quantum wells in a magnetic field has been investigated by Some and Nurmikko.[12] We used a modulation-doped parabolic well primarily as a well-characterized system to test our model of THz emission. At zero magnetic field the spectrum shows an emission feature at 2.5THz due to the intersubband plasma oscillation, as well as a second emission feature centered at 0.5THz, which we associate with photoexcitation of the substrate.[13] The relative strength of these features can be varied by changing the center-frequency of the pump laser between $\lambda = 800\text{nm}$ and $\lambda = 760\text{nm}$, and thus the fraction of the radiation absorbed in the quantum well.

The THz emission spectrum was recorded as a function of magnetic field at $\theta = 45^\circ$ to the sample surface. At high magnetic fields we observe two features associated with the quantum well. The intersubband plasma resonance is observed at all fields, and its center frequency is nearly field-independent. A second line is observed near the electron cyclotron frequency in the quantum well, $\omega_c \cos\theta$. In addition, we observe features associated with photoexcitation of the substrate. The broad feature at 0.5THz evolves with field, and at high fields we see a relatively sharp line close to the cyclotron frequency in GaAs, and a broad feature centered near 0.4THz.

We have modeled this system as two components: Quantum well electrons in a parabolic potential, plus a plasma of photoexcited free carriers in the GaAs substrate. Model emission spectra are plotted in Figure 3b. The simulation shows

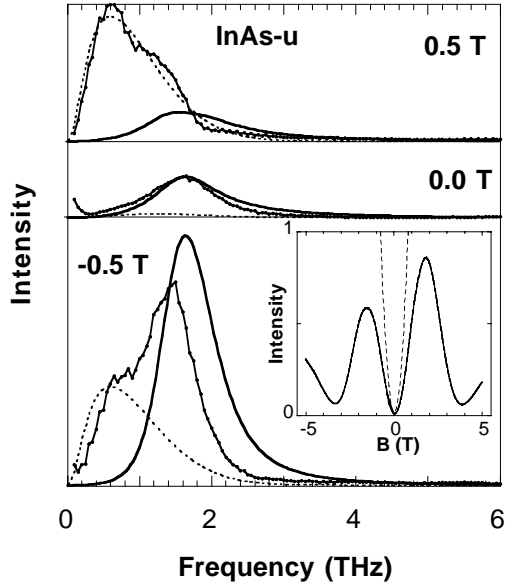


Fig. 4. THz emission spectrum of n-InAs ($n = 1.8 \times 10^{16} \text{ cm}^{-3}$) optically excited with a 12fs Ti:S laser. Points are experimental data. Solid lines are simulated emission due to extrinsic electrons. Dashed lines are simulated emission from surface accumulation layer. Inset: integrated power versus magnetic field (measured with a 140fs Ti:S laser).

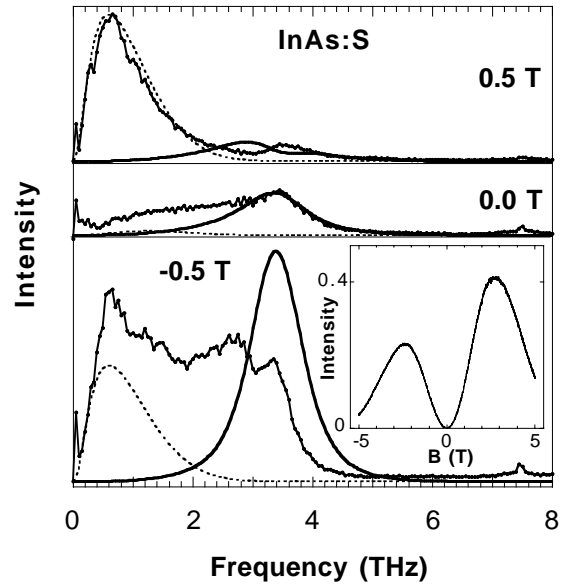


Fig. 5. THz emission spectrum of n-InAs ($n = 7.5 \times 10^{16} \text{ cm}^{-3}$) optically excited with a 12fs Ti:S laser. Points are experimental data. Solid lines are simulated emission due to extrinsic electrons. Dashed lines are simulated emission from surface accumulation layer. Inset: integrated power versus magnetic field (measured with a 140fs Ti:S laser).

two features associated with the quantum well: emission due to intersubband-plasma oscillations, and emission associated with cyclotron motion in the plane of the well. At high fields the simulation shows an avoided crossing between these modes. The model predicts three modes associated with magnetoplasma oscillations of the photoexcited carriers in the substrate: emission at the upper and lower magnetoplasma frequencies, and a third peak at the $B = 0$ plasma frequency associated with carrier motion parallel to the magnetic field. At high fields, the upper magnetoplasma frequency asymptotically approaches the cyclotron frequency.

The model qualitatively describes the experimental data, and we associate the observed quantum well features with the intersubband plasma oscillation and with in-plane cyclotron motion of the quantum well electrons. The substrate features in the spectra are also qualitatively described by the model, particularly emission at the GaAs cyclotron frequency. However, the experimental spectra do not show the predicted coupling between the quantum well modes, although the predicted anti-crossing behavior has been observed in far-infrared transmission measurements of similar samples.[14] Additionally, it does not predict the large line-broadening observed in the low-frequency emission. We suggest that the large line-width of the central peak is due to the inhomogeneous carrier density in the photoexcited plasma, which is not treated in the model. In contrast, at high fields the upper branch frequency is close to the cyclotron frequency and its position is nearly density independent. Therefore the cyclotron peak becomes narrow.

3.3 n-InAs

It is well known that the Fermi-level is pinned in the conduction-band at oxidized InAs surfaces, and magneto-transport[15] and photoelectron[16] spectroscopy have identified a surface accumulation layer with typical carrier densities of order 10^{12} cm^{-2} . There is no depletion layer at the InAs-air interface, and the surface electric field is almost completely screened by conduction-band electrons. Therefore, acceleration of photoexcited carriers in the surface field is unlikely to play an important role in THz generation in InAs. This suggestion is supported by experiment. In InAs the conduction band bends down at the surface, so that the surface electric field in n-GaAs and in n-InAs have opposite sign. Our experiments show that the initial sign of the radiated THz electric field is the same in n-GaAs and n-InAs (Figure 1). Since the sign of the field is determined by the direction of acceleration of the charge,

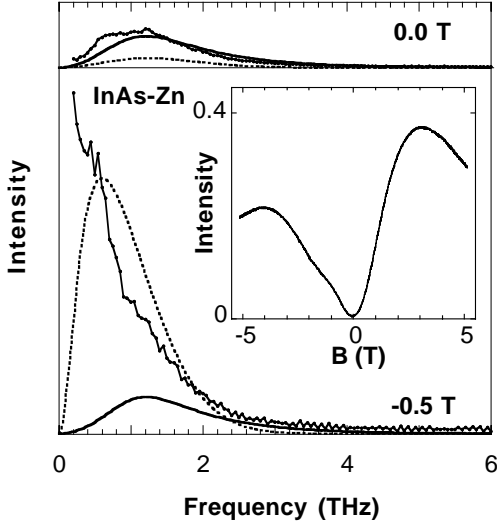


Fig. 6. THz emission spectrum of p-InAs ($p = 2 \times 10^{17} \text{ cm}^{-3}$) optically excited with a 12fs Ti:S laser. Points are experimental data. Solid lines are simulated emission due to extrinsic electrons. Dashed lines are simulated emission from surface accumulation layer. Inset: integrated power versus magnetic field (measured with a 140fs Ti:S laser).

the data are inconsistent with surface-field screening in InAs. On the other hand, photoexcitation with $\lambda=800\text{nm}$ radiation produces carriers with excess energy $\sim 1\text{eV}$ in InAs. These rapidly thermalize with the extrinsic carriers, producing a large gradient in the electron temperature near the surface, and a Demer field $\sim 40\text{kV/cm}$ through equation (1), [17] comparable to the surface electric field in GaAs with carrier densities of order 10^{16} cm^{-3} . Hot carrier diffusion drives electrons into the sample, consistent with experiment.

THz emission spectra from n-InAs are shown in Fig. 4 ($n = 1.8 \times 10^{16} \text{ cm}^{-3}$) and Fig. 5 ($n = 7 \times 10^{16} \text{ cm}^{-3}$). For both samples the $B = 0$ emission spectra is dominated by a single broad peak at the plasma frequency. All InAs samples investigated also show a sharp emission feature near the LO phonon frequency. Emission spectra and the integrated THz power from the n-type samples were recorded for magnetic fields parallel to the sample surface from $B = -5\text{T}$ to 5T . In the $n = 1.8 \times 10^{16} \text{ cm}^{-3}$ sample, the broad feature observed at $B = 0$ evolves and moves to lower frequency with increasing field. As in GaAs, we observe a change in the sign of the electric field component at the zero-field plasma frequency at a finite positive field ($B = +0.2\text{T}$). However, in InAs the emission becomes dominated by a distinct low-frequency feature which peaks near $\nu \approx 0.35 \text{ THz}$. This low frequency component changes sign at $B = 0$. We obtain similar results from the more heavily doped sample. Spectra were also measured with the magnetic field at $\theta = 45^\circ$ to the surface. In this geometry the low-frequency feature shifts to higher frequencies with increasing field.

As for the parabolic well, we use a two component system to model THz emission in InAs. We model carriers in the surface accumulation layer as a 2D-plasma, and the extrinsic carriers in the bulk as a 3-D plasma. We cannot see the intersubband plasma oscillation in the surface layer directly in our measurements: for a carrier density of $n_s \approx 10^{12} \text{ cm}^{-2}$ we expect $\omega_s \sim 15 \text{ THz}$, which is outside the experimentally accessible range. However, for B parallel to the surface, the 2D plasma model predicts emission which peaks at low frequencies due to purely damped carrier motion parallel to the surface. We fit the THz emission from InAs as a sum of surface and bulk contributions. The parameters of the bulk plasma were determined from measurements at $B = 0$. The relative amplitudes of the bulk and surface oscillations was fit from measurements at $B = 0.5\text{T}$. Figures 3 and 4 show model emission spectra from the bulk and surface carriers calculated using these parameters. The model also predicts that the low-frequency component should change sign at $B = 0$, while the high-frequency bulk-like component should change sign at a finite positive magnetic field. Both of these predictions are in agreement with the data. For a B-field at 45 degrees to the surface, we have cyclotron motion in the surface layer, and the center of the low-frequency peak should shift to higher frequency with increasing field, as observed.

For magnetic fields $|B| > 1 \text{ T}$ our model reproduces the experimental line positions, but does not accurately predict the peak intensities. In particular, the model predicts that the intensity of the surface mode contribution should increase continuously with increasing field within the measurement range. Experimentally this is not observed (see Fig. 3). The discrepancy may reflect oversimplifications of the model. We have not considered any magnetic-field dependence to the initial excitation amplitude of the surface and bulk modes, or to the damping parameters. We also have not considered coupling between surface and bulk modes.

THz emission data for p-InAs is shown in Figure 6. At finite magnetic fields the spectrum is dominated by low-frequency emission. The peak-frequency of the emission increases approximately linearly with increasing field, and at $B = 5\text{T}$ the emission is 0.84 THz and the line-width is 1.1THz (FWHM). At high fields ($B = 3\text{T}$) the radiated THz power is comparable to that emitted by the n-InAs samples.

4. SUMMARY

We report measurements of photo-induced THz emission from bulk InAs, n-GaAs and a parabolic GaAs/AlGaAs quantum well as a function of magnetic field. The emission processes in these three systems can be described using a semiclassical model of magneto-plasma oscillations of bulk free carriers and cyclotron-intersubband motion of free carriers in a 2D electron gas. These models provide a simple physical picture of the emission mechanism, but do not fully explain our results. The bulk model describes THz emission from n-GaAs at all magnetic fields. A model including both bulk plasma oscillations and THz emission from a surface accumulation layer describes THz emission from the parabolic GaAs/AlGaAs quantum well and from InAs in a moderate magnetic field, but in InAs there are significant discrepancies at fields $|B| > 1.0\text{ T}$.

ACKNOWLEDGEMENTS

This work was supported by the National Science Foundation through the NSF-RUI program (DMR-0074622) and the University of Minnesota MRSEC (DMR 98-09364). KU and TM acknowledge support from the Austrian Science Foundation (F016).

REFERENCES

1. X.C. Zhang, B.B. Hu, J.T. Darrow & D.H. Auston, Appl. Phys. Lett. **56**, 1011 (1990).
2. X.-C. Zhang, Y. Jin, L.E. Kingsley & M. Weiner, Appl. Phys. Lett. **62**, 2477 (1993).
3. N. Sarukura, H. Ohtake, S. Izumida & Z. Liu, J. Appl. Phys. **84**, 654 (1998).
4. R. McLaughlin, A. Corchia, M.B. Johnston, Q. Chen, C.M. Ciesla, D.D. Arnone, G.A.C. Jones, E.H. Linfield, A.G. Davis & M. Pepper, Appl. Phys. Lett. **76**, 2038 (2000).
5. J.N. Heyman, P. Neocleous, D. Hebert, P.A. Crowell, T. Müller & K. Unterrainer, Phys. Rev. B **64**, 085202 (2001).
6. H. Ohtake, S. Ono, M. Sakai, Z. Liu & T. Tsukamoto, Appl. Phys. Lett. **76**, 1398 (2000).
7. C. Weiss, R. Wallenstein & R. Beigang, Appl. Phys. Lett. **77**, 4160 (2000).
8. A. Corchia, R. McLaughlin, M.B. Johnston, D.M. Whittaker, D.D. Arnone, E.H. Linfield, A.G. Davies & M. Pepper, Phys. Rev. B **64**, 205204 (2001).
9. T. Dekorsky, H. Auer, H.J. Bakker, H.G. Roskos & H. Kurz, Phys. Rev. B **53**, 4005 (1996).
10. R. Kersting, K. Unterrainer, G. Strasser, H.K. Kauffmann & E. Gornik, Phys. Rev. Lett. **79**, 3038 (1997).
11. M.P. Hasselbeck, D. Stalnaker, L.A. Schlie, T.J. Rotter, A. Stintz & M. Sheik-Bahae, submitted to Phys. Rev. Lett.
12. D. Some & A.V. Nurmikko, Phys. Rev. B **50**, 5783 (1994).
13. R. Bratschitsch, T. Muller, R. Kersting & K. Unterrainer, Appl. Phys. Lett. **76**, 3501 (2000).
14. K. Karrai, H.D. Drew, M.W. Lee & M. Shayegan, Phys. Rev. B **39**, 1426 (1989).
15. D.C. Tsui, Phys. Rev. B **8**, 2657 (1973).
16. G.S. Bell, T.S. Jones & C.F. McConville, Appl. Phys. Lett. **71**, 3688 (1997).
17. The order of magnitude of the Dember field was estimated using equilibrium room-temperature values for the diffusion coefficient and the thermopower coefficient.